ELSEVIER

Nuclear Instruments and Methods in Physics Research A 440 (2000) 338–347

NUCLEAR INSTRUMENTS & METHODS IN PHYSICS RESEARCH Section A

www.elsevier.nl/locate/nima

Optical characterization of $n = 1.03$ silica aerogel used as radiator in the RICH of HERMES

E. Aschenauer[a], N. Bianchi[b], G.P. Capitani[b], P. Carter[c], C. Casalino[d], E. Cisbani[e], C. Coluzza[f], R. De Leo[d,*], E. De Sanctis[b], D. De Schepper[g], V. Djordjadze[a], B. Filippone[c], S. Frullani[e], F. Garibaldi[e], J.O. Hansen[g], B. Hommez[h], M. Iodice[e], H.E. Jackson[g], R. Kaiser[a], J. Kanesaka[i], L. Lagamba[d], V. Muccifora[b], E. Nappi[d], W.-D. Nowak[a], T.G. O'Neill[g], D. Potterveld[g], D. Ryckbosch[h], Y. Sakemi[i], F. Sato[i], A. Schwind[a], K. Suetsugu[i], T.-A. Shibata[i], E. Thomas[b], M. Tytgat[h], G.M. Urciuoli[e], K. Van de Kerckhove[h], R. Van de Vyver[h], S. Yoneyama[i], L.F. Zhang[i]

[a]*DESY Zeuthen, 15738 Zeuthen, Germany*
[b]*INFN, Laboratori Nazionali di Frascati, 00044 Frascati, Italy*
[c]*W.K. Kellog Radiation Lab, California Institute of Technology, Pasadena, CA 91125, USA*
[d]*INFN, Sezione di Bari, e Dipartimento Interateneo di Fisica, via Amendola 173, I-70126 Bari, Italy*
[e]*INFN, Gruppo Sanità, e Laboratorio di Fisica dell'Istituto Superiore di Sanità, viale Regina Elena 299, I-00161 Roma, Italy*
[f]*INFN, Sezione di Roma 1, e Dipartimento di Fisica dell'Università "La Sapienza", I-00100 Roma, Italy*
[g]*Argonne National Laboratory, Argonne, IL 60439, USA*
[h]*University of Gent, 9000 Gent, Belgium*
[i]*Department of Physics, Tokyo Institute of Technology, Tokyo 152-8551, Japan*

Received 17 June 1999; accepted 18 August 1999

Abstract

The optical properties of silica aerogel tiles with a refractive index of 1.03 and dimensions $11 \times 11 \times 1$ cm^3, produced by the Matsushita Electric Works (Japan), have been measured in the wavelength range from 200 to 900 nm. The tiles are used as one of the two radiators of the ring imaging Cherenkov counter of the HERMES experiment at DESY-HERA. The transmittance of light has been measured on 200 tiles by means of a double beam spectrophotometer. The light transflectance and reflectance have been measured on one tile by means of a single-beam spectrophotometer and an integrating reflecting sphere. Typical values of the measured transmittances at a wavelength $\lambda = 400$ nm are around 0.67. The measured transflectance increases almost linearly from 0.4 to 0.96 in the interval 200–300 nm, and remains nearly constant at the value 0.95 in the complementary λ-range. The measured reflectance, mostly confined below 400 nm, is completely interpretable as backscattering from inside the aerogel, revealing an absence of light reflection at the aerogel surfaces. The transmittance data have been fitted with the Hunt formula, whose parameters have been used to evaluate the number of unscattered and scattered Cherenkov photons produced by aerogel. For stacks of 5 tiles and quantum

* Corresponding author. Fax: + 39-080-5534938.
E-mail address: deleo@ba.infn.it (R. De Leo)

0168-9002/00/$ - see front matter
PII: S0168-9002(99)00923-7

efficiencies of phototubes with bialkali photocathodes, rings with up to 19 photoelectrons/event can be expected for $\beta = 1$ particles.

Keywords: RICH; Aerogel; Optical properties

1. Introduction

Silica aerogel, presently available with a refractive index between 1.01 and 1.1, is crucial to achieve particle separation by means of the Cherenkov effect at lower momenta where neither gases at atmospheric pressure nor liquid Cherenkov radiators are suitable.

Although the silica aerogel is often employed in threshold Cherenkov detectors, its use in a ring imaging Cherenkov counter (RICH) is quite new, and is a consequence of the improvement in light transmittance and hydrophobicity made possible by a production technique developed only recently [1,2]. The use of aerogel as radiator in a RICH was first proposed for the LHCb experiment [3,4].

The RICH of the HERMES Collaboration [5] at DESY is designed to separate pions, kaons, and protons in the momentum range from 2 to 20 GeV/c. It combines aerogel and gaseous C_4F_{10} radiators. Cherenkov photons are focussed by spherical mirrors onto an array of 1934 3/4″ Philips XP1911 photomultipliers read out digitally by a LeCroy PCOS4 system. A general description of the HERMES apparatus can be found in Ref. [6].

The aerogel employed in the RICH of HERMES has been manufactured by the Matsushita Electric Works with a new technique able to produce large volumes of aerogel with improved optical quality [1,2]. This paper reports the results of a study on the optical properties of 200 tiles of this aerogel. This paper is organized as follows. In Section 2 the variations of the refractive index, the dimensions, and the surface shape of the tiles are briefly summarized. In Section 3 the light transmittance measurements in the range of 200–900 nm for each of the 200 tiles are presented, as well as the transflectance and the reflectance measurements on one tile using an integrating reflecting sphere. In Section 4 the results for fitting the transmittance measurements with the Hunt formula are presented. In Section 5 the Cherenkov photon yield produced by this aerogel is calculated based on the deduced Hunt parameters. Finally, in Section 6 the conclusions of the paper are given.

2. Variation of the dimensions and refractive index of the aerogel tiles

Matsushita produced 1680 aerogel tiles for HERMES with the nominal dimensions $11 \times 11 \times 1$ cm^3 and refractive index 1.03. Only 1060 tiles passed the quality test which required strict limits to the variation of the refractive index (1.0293–1.0313), surface dimensions (11.31–11.51 cm), and thickness (1.025–1.230 cm), and no visible large cracks in the tile.

Tile dimensions (x, y, t) have been measured with callipers. In particular, the thickness (t) has only been measured at the edges of each tile. The refractive index (n) has been measured with a laser at 633 nm by applying the minimum deflection method at the four corners of the tiles, and assuming as final value the mean of the four measurements.

For this report 200 tiles have been randomly selected among the 1060 which passed the quality test. Fig. 1 shows the x, y, t, and n distributions of these tiles. Their mean values are 11.39 cm, 11.39 cm, 1.125 cm, and 1.0304, respectively. The relative standard deviations are 0.25%, 0.27%, 4.4% and 0.035%, respectively. These variations are due to two terms; one dependent on the position chosen in the tile for the measurement (position-dependent term), and one due to differences from tile-to-tile (position-independent term). A large spread (total width 17%) in the thicknesses of the different samples has been observed. There is no correlation between the thicknesses and the refractive indices, as shown by the scatter plot of these two quantities in Fig. 1.

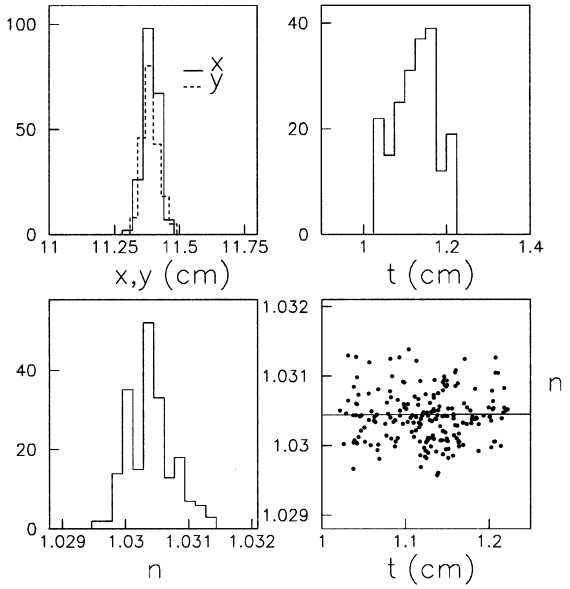

Fig. 1. The distribution of the transversal dimensions (x and y), the thickness (t), and the refractive index (n) of the 200 aerogel tiles studied in this paper. The scatter plot of the refractive indices versus the thickness including a linear fit to the experimental data.

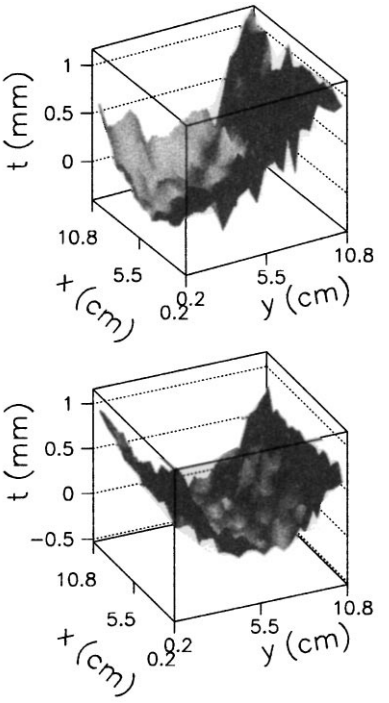

Fig. 2. Surface plots of the thickness variations over the curved surface of two aerogel tiles measured by means of a laser-based linear sensor (see text). The variations are presented relative to the thickness at the tile center.

The large spread in the tile thickness distribution suggested checking the thickness variation over the entire surface of an individual tile. Indeed an increase of the thickness at the edges of the tiles is expected due to capillary forces acting on the upper surface of the box containing the tile during its manufacture. The thickness variation over the entire upper surface of two tiles has been measured with a signal processor equipped with a laser-based linear sensor provided by Omron (Japan). To avoid reflections from the internal part of the aerogel, an aluminum plate with the size $2\times2\times0.3$ mm^3 was moved across the aerogel surface in order to reflect the laser spot. In Fig. 2 the surface plots of the thickness variations of the two tiles are shown. The variations are plotted relative to the thickness at the tile center. Differences of nearly 1.5 mm have been observed, suggesting that the detected 4.4% thickness variation of all the tiles is mostly position dependent, i.e. it is due to variation in the thickness of each single tile. Moreover, Fig. 2 suggests that the thickness variation is not localized to the edges only, but affects the entire tile surface. A visual inspection of the tiles confirms that they all have one flat and one inside-curved surface, the latter being thinner at the tile center.

As a consequence, it is deduced that the tile thickness measurement at the edges is only a rough estimation. The mean thickness at the center of the tiles, surely smaller than the value at the edges, has been assumed as 1 cm in Section 5.

3. Optical measurements

A crucial optical property of a RICH radiator is that it minimizes scattering, absorption, and reflection of photons produced in the medium. In fact, any angular dispersion caused by the radiator medium would harm the precision obtainable in the determination of the Cherenkov angle.

The combined processes of absorption, scattering, and reflection influence the "transmittance" (T), which accounts for the residual light from aerogel in the forward direction. In order to disentangle reflection, absorption, and scattering it is necessary to measure also the "transflectance" (TF) and "reflectance" (R). TF is the fraction of light emerging in all directions from the sample, and is linked to the "absorbance" ($\mathscr{A}$) through the simple equation: $TF = 1 - \mathscr{A}$. R is the fraction of light emerging in the backward direction.

T is usually measured by a spectrophotometer. Linear-type spectrophotometers permit measurement of T's even through samples of large dimensions, like our aerogel tiles. TF and R can be measured by a spectrophotometer used with an "integrating reflecting sphere". The commercially available spheres can only measure TF's for samples of few cubic centimeters.

3.1. Transmittance measurements

The transmittances for the 200 aerogel tiles have been measured with a linear-type double beam LAMBDA-3B spectrophotometer (Perkin-Elmer company) from 200 to 900 nm in steps of 10 nm. The systematic error in the transmittance measurements has been estimated by interchanging sample and reference beams. It resulted in around 0.5% below 320 nm, and less than 0.1% in the rest of the λ-range. Sample and reference beams are each defined by two 1.8×1.1 cm^2 slits placed at the entrance and exit of the sample holder. The wavelength calibration of the spectrophotometer has been checked by observing the transmittance plot of a reference holmium oxide sample, and was found to be better than 1 nm over the whole λ-range.

In Fig. 3 the highest and the lowest transmittance curves obtained by measuring the 200 tiles are reported. The light impinged on each tile at the same surface position nearly in the center. The spectra obtained for the other 198 tiles are similar and lie between these two extremes.

To estimate the statistical accuracy of transmittance, the measurement at the same position in the same tile has been repeated several times. This was done for three different wavelengths assumed as reference (250, 400, and 800 nm), as reported in Fig. 4 (left column).

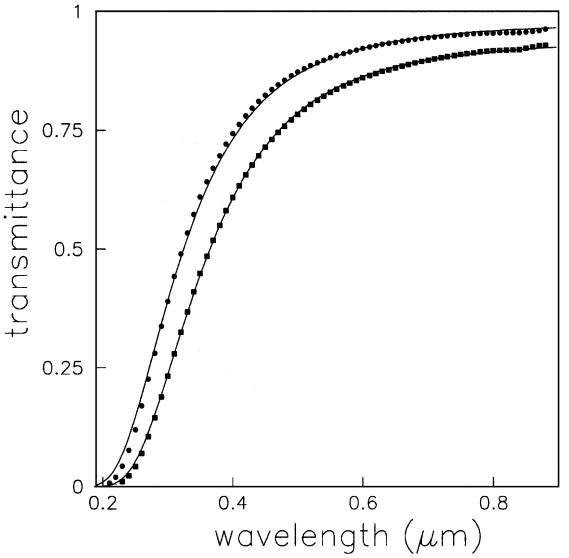

Fig. 3. The highest and lowest transmittance curves (points), measured in steps of 10 nm between 200 and 900 nm, from those 200 examined aerogel samples. The solid lines are fits to the experimental data based on Eq. (4).

The dependence of the transmittances on the position in the tile has been evaluated by repeating the measurement at 40 different positions in the central part of the tile, each position spaced 1 cm apart. Fig. 4 (central column) depicts the distribution of the measured transmittances.

The transmittance distributions at the three reference wavelengths for the 200 aerogel tiles measured at the same central position (6 cm from one corner along the diagonal) are reported in the right column of Fig. 4. The mean values of T at these wavelengths are 0.070, 0.675, and 0.941, respectively.

The standard deviations of the distributions in Fig. 4, reported in Table 1, suggest that the contribution of the position-dependent term is low at 250 nm where T is small, but becomes the dominant one when the transmission is higher.

3.2. Transflectance measurements

The transflectance has been measured on small pieces with surfaces of roughly 1.5×3 cm^2 that

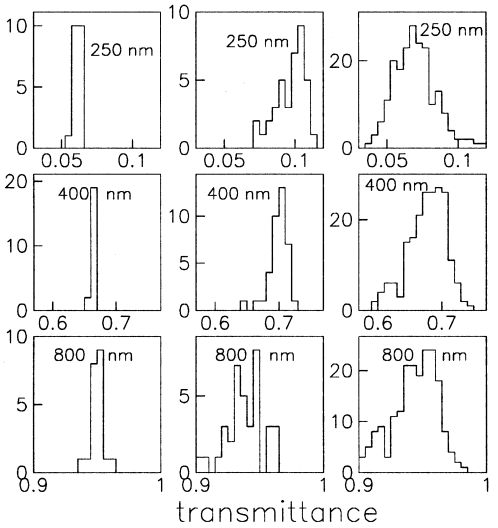

Fig. 4. The distributions of the transmittances at the three indicated wavelengths, for one sample measured at the same position (left column), for another sample measured at 40 different positions (central column), and for the 200 aerogel tiles measured at the same position of each tile (right column).

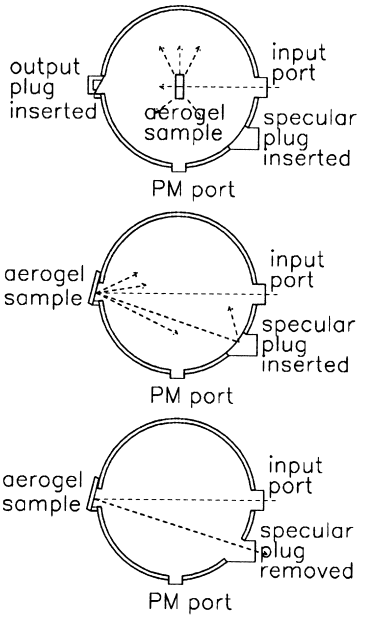

Fig. 5. The integrating sphere equipped for transflectance (upper panel), total reflectance (central panel), and diffusive reflectance (lower panel) measurements.

Table 1
Standard deviations of transmittance distributions

λ (nm)	Statistical (%)	Position-dependent (%)	Tile-to-tile (%)
250	2.3	10.2	20.9
400	0.6	1.9	4.8
800	0.5	2.1	2.3

resulted from one broken tile. It is important to stress that the pieces were not machined on their lateral surfaces to prevent any mechanical processes altering the absorption of light in the samples. Each piece was placed in an integrating sphere (from LabSPHERE) covered internally with Spectralon, a material with high- and near-Lambertian reflectivity. The transflectance is determined as the ratio between the measurements of light collected by the sphere with and without the sample. The light in the sphere was supplied by a CARY-5 spectrophotometer (Varian company) in the 200–900 nm wavelength range in steps of 1 nm. In transflectance measuring mode the sphere is equipped with only two small holes: one for the entrance of the light and one for the photomultiplier (see the upper panel of Fig. 5). The systematic error in the TF measurements was obtained by repeating the calibration procedures and has been found to decrease from 5% to 1.5% in the interval from 200 to 400 nm, to be around 1.5% between 400 and 700 nm, and around 2.5% above.

In Fig. 6 one of the measured transflectances (all others are very similar) is reported together with the transmittance for the same tile. The transflectance shows a steep increase between 200 to 300 nm, and a nearly flat region from 300 to 900 nm.

The transflectance is directly linked to the absorption length Λ_A:

$$\mathrm{TF} = \mathrm{e}^{-t/\Lambda_A} \tag{1}$$

while the transmittance is also linked to the scattering length Λ_S, and hence to the attenuation length Λ:

$$T = \mathrm{e}^{-t(1/\Lambda_A + 1/\Lambda_S)} = \mathrm{e}^{-t/\Lambda}. \tag{2}$$

The absorption and scattering lengths can be determined from the two experimental curves in

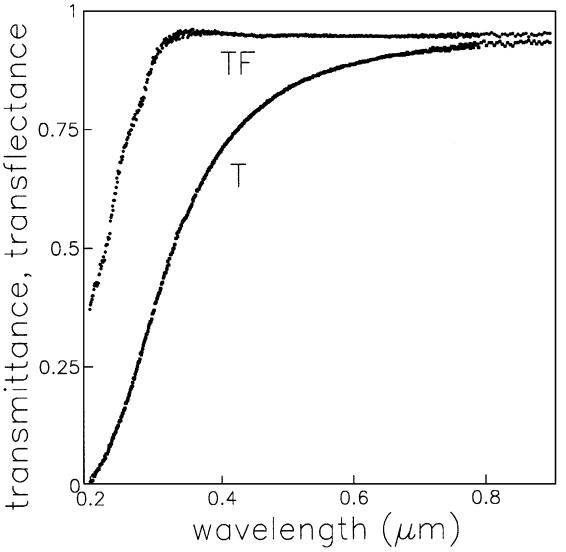

Fig. 6. Typical measured transflectance (TF) and transmittance (T) for a wavelength range between 200 and 900 nm in steps of 1 nm.

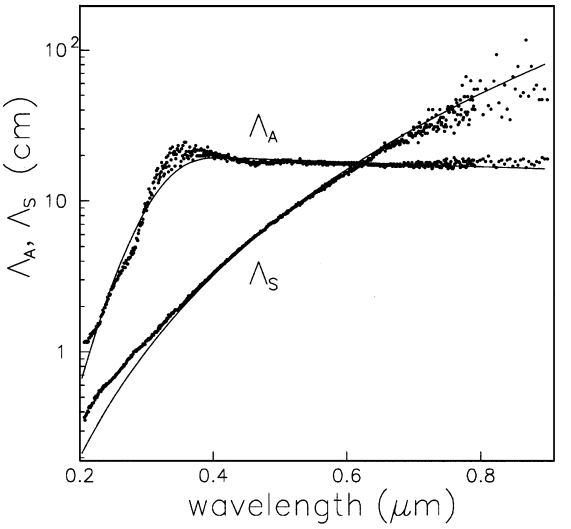

Fig. 7. The absorption and scattering lengths determined from the transflectance and transmittance measurements reported in Fig. 6. The fit to Λ_S assumes a const λ^4 function, the fit to Λ_A a complex λ-dependence function.

Fig. 6 and Eqs. (1) and (2), as shown in Fig. 7. Scattering is the dominant process up to 600 nm, absorption dominates from 650 to 900 nm. In this interval the observed absorption length has a value around 20 cm, which is low compared to that previously reported [7] for other aerogel and measured with a different equipment.

Above 350 nm the scattering length is well fitted by a λ^4-dependence (see the curve on Λ_S in Fig. 7), while the absorption length shows a λ^8-dependence around 250 nm, and is nearly constant in the rest of the interval.

3.3. Reflectance measurements

The light reflected or backscattered from one aerogel tile has been measured with the same integration sphere by positioning the sample at the exit of the sphere, in place of the output Spectralon plug. This aperture has its normal at 7° from the sphere axis (light path), thus allowing to displace the specular reflected beam from the incident one, and to hit the sphere internally at the position of the specular Spectralon plug, as shown in the central panel of Fig. 5.

The reflectance measured with the specular plug in place is shown in the upper plot of Fig. 8. Nearly half of the beam intensity is reflected or backscattered at lower wavelengths. However, the reflectance measured with the specular plug removed is identical to the one measured with the plug inserted. The difference between the two measurements is shown in the second panel of Fig. 8. The difference is less than 0.1% and practically zero within the fluctuations in the full λ-range. This proves the absence of specular reflection in aerogel, as expected by the Fresnel's law and from its very low refractive index.

Diffusive reflection (observing the cosine Lambert's law) is also negligible for aerogel. In fact, the full incident laser beam intensity has been obtained by summing over the specular reflected and transmitted beam intensities for light that was directed onto a thin piece of aerogel under angles between 75° and 87°, an angular range where specular reflection is no longer absent.

The same conclusions can be drawn from the last two panels of Fig. 8, which show that the measured reflectance is completely due to backscattering. This last quantity has been calculated from the

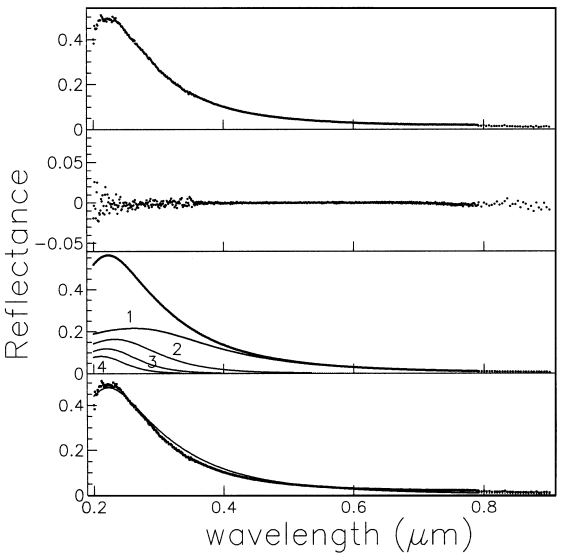

Fig. 8. (Top panel) The measured reflectance of light from aerogel. (Second panel) The difference between the reflectances measured with and without the specular plug in the integrating sphere. (Third panel) Calculated fraction of backscattered photons from aerogel together with their fractions suffering 1, 2, 3, and 4 scatterings. (Fourth panel) The measured reflectance (the same as the top panel) from aerogel with the calculated backscattering of the third panel of the figure renormalized with a factor 0.85.

values of Λ, Λ_S, and Λ_A in Fig. 7. It is shown in the third panel of Fig. 8 together with the fractions R_1, R_2, R_3, and R_4 of photons diffused in the backward direction by 1, 2, 3, or 4 scatterings, respectively:

$$
\begin{aligned}
R_1 &= \frac{\Lambda}{4\Lambda_S}(1-\mathrm{e}^{-2t/\Lambda}),\\
R_2 &= \frac{1}{2}\left(\frac{\Lambda}{\Lambda_S}\right)^2\left(1-\mathrm{e}^{-t/\Lambda}-\frac{1-\mathrm{e}^{-2t/\Lambda}}{2}\right),\\
R_3 &= \frac{1}{2}\left(\frac{\Lambda}{\Lambda_S}\right)^3\left[\left\{1-\mathrm{e}^{-t/\Lambda}\left(1+\frac{t}{\Lambda}\right)\right\}\right.\\
&\qquad \left.+\frac{1-\mathrm{e}^{-2t/\Lambda}}{2}-(1-\mathrm{e}^{-t/\Lambda})\right],\\
R_4 &= \frac{1}{2}\left(\frac{\Lambda}{\Lambda_S}\right)^4\left[\left\{-\frac{1}{2}\mathrm{e}^{-t/\Lambda}\left(\frac{t}{\Lambda}\right)^2\right\}-\frac{1-\mathrm{e}^{-2t/\Lambda}}{2}\right.\\
&\qquad \left.+(1-\mathrm{e}^{-t/\Lambda})\right]. \qquad (3)
\end{aligned}
$$

The calculated backscattering has to be reduced to consider the effective solid angle from the aerogel to the sphere. The lowest plot of Fig. 8 shows that the calculated backscattering, renormalized with a fitted factor of 0.85, agrees nicely with the measured reflectance over the full λ-range.

From the previous results it can be deduced that both the specular and diffusive reflected light from aerogel is negligible for all wavelengths in this study. For this reason it has not been considered in the analysis of the measured transmittances.

4. Hunt parameters

The transmission in aerogel is usually parameterized [8] by means of the following equation (Hunt formula):

$$T = A\mathrm{e}^{-Ct/\lambda^4} \qquad (4)$$

which assumes that the scattering cross section varies with λ^{-4} (Rayleigh scattering), and that the absorption process, represented by A, is independent of λ. In this case A is equal to the transflectance TF of Eq. (1). These assumptions are corroborated by the results in Fig. 7, at least for wavelengths above 300 nm. The fits to the transmittances, based on Eq. (4), are shown as solid lines in Fig. 3.

The clarity coefficient C (usually measured in $\mu m^4/cm$ units), is proportional to the radiation which is scattered/unit of sample length, while the quantity $1-A$ describes the light absorbed ($1-A=\mathscr{A}$) in the sample. C and A are called the Hunt parameters. Tiles with a good optical quality have values for A and C close to 1 and 0, respectively.

Due to the uncertainties in the thickness of the tiles, in the discussion which follows Ct, the total scattering produced by the tiles, will be considered, rather than C, the scattering per unit of length.

The distributions of the Hunt parameters (A and Ct) deduced for all 200 tiles are reported in the upper panels of Fig. 9. Their mean values and standard deviations (σ) are given in Table 2. In the lower panels of Fig. 9 the distributions of the Hunt parameters obtained from 40 transmittance curves measured at different positions of the central part of one tile are reported. The standard deviations of these last two distributions, reported in the last

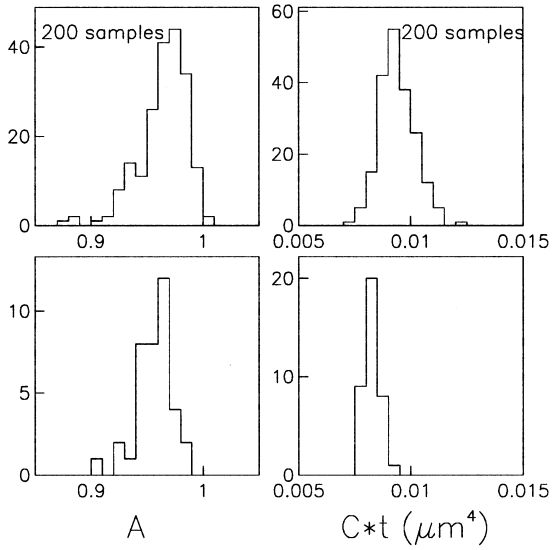

Fig. 9. The distribution of the Hunt parameters A (left side) and Ct (right side) obtained from the transmittance curves of the 200 aerogel samples (top panels of the figure), and from 40 transmittance measurements in different positions of the central part of one tile (lower panels).

Table 2
Mean values of Hunt parameters and their standard deviations

Hunt parameter	Average value	σ (%)	σ_{pos} (%)
A	0.964	2.4	1.8
Ct (μm^4)	0.0094	8.3	8.3

column of Table 2, can be assumed as the position dependent part (σ_{pos}) of the standard deviation of the 200 tiles. From Table 2 it is deduced that the standard deviation of A is nearly half position independent (due to variations from tile-to-tile), and half position dependent (due to variation in the same tile), while most of that of Ct is position dependent.

5. Unscattered and scattered Cherenkov photons

The number of unscattered Cherenkov photons produced in a stack of m aerogel tiles, each of thickness t, has been evaluated assuming particles crossing the stack perpendicularly, an uniform production of Cherenkov photons, and considering their probability to survive while propagating through the aerogel from the production point to the exit surface:

$$\frac{dN_{unsc}}{d\lambda} = \frac{2\pi\alpha}{\lambda^2}\left(1-\frac{1}{\beta^2 n^2}\right)t\int_0^m (Ae^{-Ct/\lambda^4})^{(m-x)/\cos\theta}\,dx. \tag{5}$$

Here θ is the polar Cherenkov emission angle measured from the particle direction ($\cos\theta = 1/n\beta$), β is the particle velocity.

For $\beta = 1$ particles one gets

$$\frac{dN_{unsc}}{d\lambda} = \frac{2\pi\alpha}{\lambda^2}\left(1-\frac{1}{n^2}\right)t[1-(Ae^{-Ct/\lambda^4})^{mn}] \times \frac{1}{\{-\ln(A)+Ct/\lambda^4\}n}. \tag{6}$$

In a similar way, the number of Cherenkov photons absorbed in the stack is evaluated:

$$\frac{dN_{abs}}{d\lambda} = \frac{2\pi\alpha}{\lambda^2}\left(1-\frac{1}{n^2}\right)t\left[m-\frac{1}{-\ln(A)n}(1-A^{mn})\right] \tag{7}$$

and the number of Cherenkov photons scattered from their primary θ direction:

$$\frac{dN_{sc}}{d\lambda} = \frac{2\pi\alpha}{\lambda^2}\left(1-\frac{1}{n^2}\right)t\left[\frac{1}{-\ln(A)n}(1-A^{mn}) - \{1-(Ae^{-Ct/\lambda^4})^{mn}\}\frac{1}{\{-\ln(A)+Ct/\lambda^4\}n}\right]. \tag{8}$$

The upper panel of Fig. 10 shows the wavelength dependence of unscattered and scattered Cherenkov radiation produced in a stack of $m = 5$ tiles with a total thickness of 5 cm.

The λ-dependence of the number of photoelectrons produced by these distributions is reported in the lower panel of Fig. 10. These calculations include the typical quantum efficiency (see the dot-dashed curve) of bialkali photocathodes fully covering the focal plane (dead areas among photomultipliers are not considered).

The two panels of Fig. 10 show three similar curves: the central, upper and lower similar curves are calculated by using, respectively, the mean Hunt parameters and the values obtained from these by adding or subtracting one standard deviation.

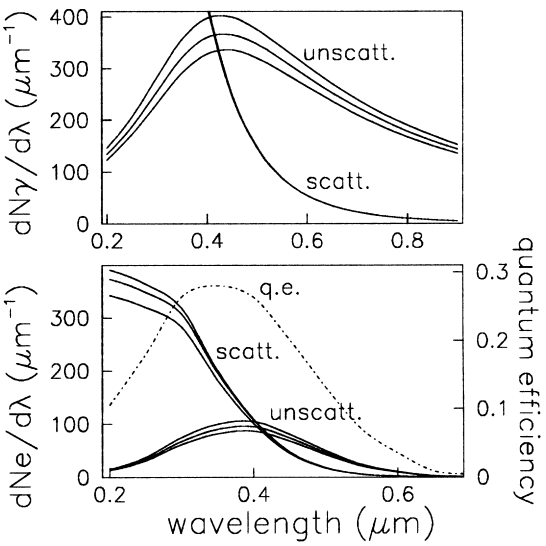

Fig. 10. (Upper panel) Distribution in wavelength of unscattered and scattered Cherenkov radiation produced in a stack (5 cm) of 5 aerogel ($n = 1.0304$) tiles here examined, and calculated from Eqs. (6) and (8). (Lower panel) The number of photoelectrons versus the wavelength deduced from the curves in the upper panel of the figure using the typical quantum efficiency of bialkali photocathodes of phototubes (dot-dashed curve). In both panels, the three similar central, upper and lower curves have been obtained by using the average values of the Hunt parameters and by adding or subtracting one standard deviation.

The integral of the "unscattered" curve in the lower panel of Fig. 10 gives the estimated number of photoelectrons. A value of 19 ± 2 is obtained in full agreement with the experimental value measured [9] for aerogel, similar to that examined here, produced by a group of the KEK-Lab. Variations due to a spread in particle velocities and incident angles on the aerogel have not been considered. Effects outside the aerogel of the actual HERMES RICH which reduce the number of photoelectrons, like the exit window of the aerogel container, the C_4F_{10} gas, mirror and photomultiplier glass reflectivity, geometrical efficiency of the mirror and photomultipliers, and the efficiency of the readout system also have been ignored. For the HERMES RICH all these effects are estimated to reduce the number of photoelectrons to 11–14 depending on the incident angle of the particles on the aerogel.

There are several photoelectrons from scattered radiation. Their polar angle is random, thus their number is noticeably reduced due to geometrical acceptance, which is not considered here.

6. Conclusions

This paper presents the measurements of light transmittance, transflectance, and reflectance in the 200–900 nm region for 1 cm thick, $n = 1.03$, aerogel tiles produced by the Matsushita Company for the HERMES RICH.

At 400 nm an average transmittance of 0.675 with a relative standard deviation of 4.8% has been measured.

The measured transflectance is strongly increasing in the interval 200–300 nm, and remains nearly constant between 300 and 900 nm.

The light specularly reflected from this aerogel has been measured to be negligible over the entire λ-range. Also the diffusive reflection has been estimated to be negligible since the measured reflectance is totally described by backscattering from inside the aerogel.

The aerogel tiles show a large thickness variation along one of their surfaces. Due to capillary effects during the tile manufacture, differences as large as 1.5 mm can be present between the center and the border of the tiles. Due to this thickness uncertainty, only the total absorption and scattering of the tiles can be extracted, rather than their values per unit of length. Absorption and scattering have been evaluated by fitting the measured transmittances with the Hunt formula, which assumes an absorption independent of λ. The average absorption (A) and scattering (Ct) Hunt parameter values (standard deviations) of the tiles are 0.964 (2.4%), and 0.0094 μm^4 (8.3%), respectively.

With the deduced set of Hunt parameters, the number of photoelectrons per event expected in the HERMES RICH using stacks of five aerogel tiles (nearly 5 cm) and typical quantum efficiencies of bialkali photocathodes has been calculated. By considering only the uncertainties affecting the evaluated Hunt parameters, this number results in 19 ± 2 photoelectrons. Variations due to a spread in particle velocities and incident angle on aerogel, and other effects absorbing Cherenkov photons in between the aerogel and the photocathode are

estimated to decrease to 11–14 the expected number of photoelectrons.

Acknowledgements

The support from Monbusho, JSPS, and Toray Science Foundation (JAPAN) is kindly acknowledged.

References

[1] I. Adachi et al., Nucl. Instr. and Meth. A 355 (1995) 390.
[2] H. Yokogawa, M. Yokoyama, J. Non-Cryst. Solids 186 (1995) 23.
[3] The LHC-B Collaboration, Status and plan of R&D for the RICH detector of LHC-B CERN/LHCC, 96–38.
[4] T. Ypsilantis, J. Seguinot, Nucl. Instr. and Meth. A 368 (1995) 229.
[5] E. Cisbani et al., HERMES Internal Note 97-005.
[6] K. Ackerstaff et al., HERMES collaboration, Nucl. Instr. and Meth. A 417 (1998) 230.
[7] A. Buzykaev, A. Daniluk, S. Ganzhur, T. Gorodetskaya, E. Kravchenko, A. Onuchin, A. Vorobiov, Nucl. Instr. and Meth. A 379 (1996) 465.
[8] L.W. Hrubesh, Optical Characterization of Silica Aerogel Glass, U.C.R.L. Report no. 53794, 1987.
[9] R. De Leo et al., Nucl. Instr. and Meth. A 401 (1997) 187.